

# Cross Correlate Tidal Reconstructed 21cm Signal with Kinematic Sunyaev-Zel'dovich Effect: A New Probe for Missing Baryons at $z \sim 1 - 2$

Dongzi Li,<sup>1,2</sup> Hong-Ming Zhu,<sup>3,4</sup> Ue-Li Pen,<sup>5,6,7,1</sup> and Yu Yu<sup>8</sup>

<sup>1</sup>*Perimeter Institute for Theoretical Physics, 31 Caroline St. N., Waterloo, ON, N2L 2Y5, Canada*

<sup>2</sup>*University of Waterloo, 200 University Ave W, Waterloo, ON, N2L 3G1, Canada*

<sup>3</sup>*Key Laboratory for Computational Astrophysics, National Astronomical Observatories, Chinese Academy of Sciences, 20A Datun Road, Beijing 100012, China*

<sup>4</sup>*University of Chinese Academy of Sciences, Beijing 100049, China*

<sup>5</sup>*Canadian Institute for Theoretical Astrophysics, 60 St. George Street, Toronto, Ontario M5S 3H8, Canada*

<sup>6</sup>*Dunlap Institute for Astronomy and Astrophysics, 50 St. George Street, Toronto, Ontario M5S 3H4, Canada*

<sup>7</sup>*Canadian Institute for Advanced Research, CIFAR Program in Gravitation and Cosmology, Toronto, Ontario M5G 1Z8, Canada*

<sup>8</sup>*Key laboratory for research in galaxies and cosmology, Shanghai Astronomical Observatory, Chinese Academy of Sciences, 80 Nandan Road, Shanghai 200030, China*

(Dated: May 5, 2016)

We propose a new way to study baryon abundance and distribution at mid redshift. We cross correlate density field from HI 21cm intensity mapping with temperature anisotropy of Cosmic Microwave Background(CMB) caused by radial motion of free electrons, i.e. kinetic Sunyaev-Zel'dovich(kSZ) effect. We put forward a 3D cosmic tidal reconstruction to recover the modes lost in 21cm foregrounds, which will effectively promote the appearance of correlation signals.

We verify the idea with simulation outputs on  $z = 1$ ,  $z = 2$ , taking into account of foreground noises, facility resolutions, and redshift distortions. We successfully recover  $> 90\%$  information of the 21cm density field at  $k \sim 0.01h/\text{Mpc}$  after tidal reconstruction. We obtain a  $r > 0.6$  correlation with origin kSZ signal from  $l \sim 100 - 2000$ . Assuming the noise level of Planck, the S/N will exceed 3 from  $l \sim 500 - 3000$ .

This is a very promising probe to study diffused matter distribution. 1. It is less biased towards local density contraction, thanks to the kinetic nature of kSZ signals; 2. It has precise redshift information from 21cm spectrum; 3. It is rather feasible to get required data of higher redshifts with large sky coverage. The 21cm intensity mapping survey has huge advantage on survey speed, facility requirements and costs comparing to spectroscopic galaxy survey.

Consider the simulated S/N level, data requirements, current and upcoming 21cm intensity mapping facilities, we are optimistic about the new probe.

PACS numbers:

## I. INTRODUCTION

While the baryon abundance of early universe is well fixed by the cosmic microwave background (CMB), Big Bang Nucleosynthesis and Lyman- $\alpha$  forest [1][2][3][4], a deficiency was noticed in local universe. At  $z \lesssim 2$  the detected baryon content in collapsed objects, eg. galaxies, galaxy clusters and groups, only account for 10% of the predicted amount. More baryons are believed to reside in Warm-Hot Intergalactic Mediums (WHIM) with typical temperature of  $10^5$  K to  $10^7$  K [5], which is too cold and diffuse to be easily detected. Continuous effort has been made to detect this part of the baryons. One common approach is using hydrogen and metal absorption lines(eg. HI, Mg II, Si II, C II, Si III, C III, Si IV, O VI, O VII) [6][7]. However, the lines are usually limited to close circumgalactic medium, while at least 25% of the baryons are believed to reside in more diffused region [8]. Moreover, the uncertainty in metallicity would sometimes reduce the reliability.

A promising tool to probe the missing baryon is the kinetic Sunyaev-Zel'dovich(kSZ) effect [9][10], an effect that is greatly known for its potential to explore the Epoch of Reionization [11][12][13]. It refers to the secondary temperature anisotropy in CMB caused by radial motions of free electrons, which only correlates to electron density and velocity, regard-

less the temperature and pressure. Since the velocity field mainly results from large scale structure, the method is less biased towards hot, compact place, and provide more information on the fraction of diffused baryons.

Attractive as it is, due to the contamination from primary CMB and residual thermal SZ signal it is difficult to filter the kSZ signal without other sources. Worse still, the signal itself does not contain redshift information.

To fix this, previous approaches cross correlated it with galaxy surveys, eg. using pairwise-momentum estimator [14] or velocity-field-reconstruction estimator [15][16]. However since they all require spectroscopy of galaxies to provide accurate redshift, the sky volume and redshift range to apply the method is limited. A recent effort try to fix this by using photometries of infrared-selected galaxies. However, since they used projected fields of the galaxies, they could only obtain a rough estimate over a wide redshift bin [17].

In this paper we present a new cross relating source, HI density field, from 21cm intensity mapping, a kind of surveys that provide integrated signals of diffuse 21cm spectra, rather than detecting individual objects.

It will make it feasible to probe the baryon content to  $z \gtrsim 1$  in very near future, with ongoing experiments like CHIME [18], Tianlai [19], HIRAX [20] etc. Besides, the 21cm spectrum contains accurate redshift information, which makes it a

good candidate to be cross correlated to kSZ signals.

This powerful probe was rarely harnessed in this topic previously, because the continuum foregrounds in 21cm measurements is typically  $10^2 - 10^3$  times brighter than cosmological signals, almost completely bury the distribution of large scale structures in radial direction, i.e. modes with small  $k_{\parallel}$ . Meanwhile the velocity field is closely related with the large scale structure, which makes the correlation difficult to see.

To compensate that, a new method called *cosmic tidal reconstruction* has been developed recently [21][22]. It can reconstruct the large scale density field from the alignment of small scale cosmic structures. In this paper, we further extend the previous 2D tidal reconstruction to 3D—this is a necessity since we need more accurate large scale density field on  $z$  directions. We discuss the influence of redshift distortions for that.

Applying this methods to foreground substracted 21cm density fields, we obtain a sufficiently good cross-correlation signal with original kSZ signals.

The paper is organized as follows. In section II, we present the complete procedure: in II A, we introduce 3D tidal reconstruction method; in II B, we describe how to cross correlate kSZ signals with reconstructed fields; In section III, we present the simulations: in III A, We address simulation setups; in III B, we demonstrate simulations results; Section IV is for error analysis and discussions: in IV A, we estimate the statistical error; in IV B, we take into account redshift distortions; in IV C, we discuss the importance of 3D tidal reconstruction; We give conclusions and discuss future applications in section V.

## II. RECONSTRUCTION ALGORITHM

### A. 3D Cosmic Tidal Reconstruction

While a cosmic signal in 21cm measurement is of the order of mK, foregrounds coming from Galactic emissions, telescope noise, extragalactic radio sources and Radio recombination lines, can reach the order of Kelvin [23][24]. Lots of techniques have been developed to substract the foregrounds, taking advantage of the attribute that they have fewer bright spectral degrees of freedom[25]. Unfortunately, the substruction usually contaminates the smooth large scale structure information. Since the large scale information is essential for the estimate of peculiar velocity, we need to recover the information. However, since large scale structure is correlated closely to the emergence of peculiar velocity, we need a method to estimate its distribution.

The cosmic tidal reconstruction is a kind of quadratic statistics developed to achieve this goal. Its main idea is using small scale filamentary structures to solve for the large scale tidal shear and gravitational potential.

Here, we present a 3 dimensional reconstruction algorithm that works best in close linear regions.

First, we filter for the small scale structures that are most likely to be influenced by tidal force of large scale fields.

(1) Convolve the field with a Gaussian kernel  $S(\mathbf{k}) = e^{-k^2 R^2/2}$ , we take  $R = 1.25 \text{ Mpc}/h$  [21], to reduce the complicated non-linear effects on small scales.

(2) Gaussianize the field, taking  $\delta_g = \ln(1 + \delta)$ . This is to allieviate the problem that filter  $W_i$  in (3) heavily weights high density regions.

(3) Apply filter  $W_i(\mathbf{k})$ , which assigns weights to  $\delta_g$  according to predicted displacements caused by tidal field in near linear regions [22].  $\delta_g^{w_i}(\mathbf{k}) = W_i(\mathbf{k})\delta_g(\mathbf{k})$ ,

$$W_i(\mathbf{k}) = i \left( \frac{P(k)f(k)}{P_{tot}^2(k)} \right)^{\frac{1}{2}} \frac{k_i}{k} \quad (1)$$

$i$  indicates  $\hat{x}, \hat{y}, \hat{z}$  directions,  $P_{tot} = P + P_{noise}$  is observed matter powerspectrum,  $P$  is theoretical matter powerspectrum,  $f = 2\alpha(\tau) - \beta(\tau)d\ln P/d\ln k$ , where  $\alpha$  and  $\beta$  are functions related to linear growth function, and are calculated to be (0.6, 1.3) for  $z = 1$  and (0.4, 0.9) for  $z = 2$ .<sup>1</sup>

Second, we estimate the tidal force and hence reconstruct the large scale density field.

(1) Following gravitational lensing procedures, we decompose the  $3 \times 3$  symmetric, traceless tidal force tensor into 5  $\gamma$  components, and estimate them from density variance.

$$\begin{aligned} \hat{\gamma}_1(\mathbf{x}) &= [\delta_g^{w_1}(\mathbf{x})\delta_g^{w_1}(\mathbf{x}) - \delta_g^{w_2}(\mathbf{x})\delta_g^{w_2}(\mathbf{x})], \\ \hat{\gamma}_2(\mathbf{x}) &= [2\delta_g^{w_1}(\mathbf{x})\delta_g^{w_2}(\mathbf{x})], \\ \hat{\gamma}_x(\mathbf{x}) &= [2\delta_g^{w_1}(\mathbf{x})\delta_g^{w_3}(\mathbf{x})], \\ \hat{\gamma}_y(\mathbf{x}) &= [2\delta_g^{w_2}(\mathbf{x})\delta_g^{w_3}(\mathbf{x})], \\ \hat{\gamma}_z(\mathbf{x}) &= [(2\delta_g^{w_3}(\mathbf{x})\delta_g^{w_3}(\mathbf{x}) - \delta_g^{w_1}(\mathbf{x})\delta_g^{w_1}(\mathbf{x}) - \delta_g^{w_2}(\mathbf{x})\delta_g^{w_2}(\mathbf{x}))]/3, \end{aligned} \quad (2)$$

(2) Reconstruct 3D density field.

$$\begin{aligned} \kappa_{3D}(\mathbf{k}) &= \frac{1}{k_1^2 + k_2^2 + k_3^2} [(k_1^2 - k_2^2)\gamma_1(\mathbf{k}) + 2k_1k_2\gamma_2(\mathbf{k}) \\ &\quad + 2k_1k_3\gamma_x(\mathbf{k}) + 2k_2k_3\gamma_y(\mathbf{k}) + (2k_3^2 - k_1^2 - k_2^2)\gamma_z(\mathbf{k})]. \end{aligned} \quad (3)$$

Third, we correct bias and suppress noise with a Wiener filter. Due to the foregrounds, the noise in  $z$  direction will be different from  $x, y$  direction, therefore we apply an anisotropic Wiener filter.

$$\hat{\kappa}_c(\mathbf{k}) = \frac{\kappa_{3D}(\mathbf{k})}{b(k_{\perp}, k_{\parallel})} W(k_{\perp}, k_{\parallel}), \quad (4)$$

Bias  $b = \frac{P_{\kappa 3D}\delta}{P_{\delta}}$ , Wiener filter  $W = \frac{P_{\delta}}{P_{\kappa 3D}/b^2}$ .

Here and afterwards, we use “ $\wedge$ ” to denote reconstructed fields.

### B. Velocity Reconstruction and kSZ signals

Due to the cancellation of positive and negative velocity, direct cross correlation between kSZ signal and density field is

<sup>1</sup> The effect of the filter  $W_i$  on different scales could be seen in Appendix 1.

hard to see. Therefore, we first estimate the peculiar velocity from the 3D density field, then construct the 2D map of kSZ signal, and correlate it with the real kSZ signal [15].

Detailed steps are as follows.

(1) Estimate the velocity field:

In linear region, the continuity equation goes like:  $\dot{\delta} + \nabla \cdot \mathbf{v} = 0$ , where  $\mathbf{v}$  is the peculiar velocity and  $\delta$  is the matter overdensity.

Therefore, we obtain an estimator of velocity distribution:

$$\hat{v}_z(\mathbf{k}) = iaH \frac{d \ln D}{d \ln a} \delta(\mathbf{k}) \frac{k_z}{k^2} \quad (5)$$

where  $D(a)$  is the linear growth function.

$v_z \propto \frac{k_z}{k^2}$ , indicating the most prominent signal comes from small  $k$  mode, which corresponds to large scale structure. This further verify our motivation for tidal reconstruction procedure.

(2) suppress the noise in velocity field with a new Wiener filter, following identical procedure as Eq.(4). This is because the term  $\frac{k_z}{k^2}$  in Eq.(5) will strongly amplify noises in small  $k$  modes.

(3) Calculate 2D kSZ map.

The CMB temperature fluctuations caused by kSZ effect is:

$$\Theta_{kSZ}(\hat{n}) \equiv \frac{\Delta T_{kSZ}}{T_{CMB}} = -\frac{1}{c} \int d\eta g(\eta) \mathbf{p}_{\parallel}, \quad (6)$$

where  $\eta(z)$  is the comoving distance at redshift  $z$ ,  $g(\eta) = e^{-\tau} d\tau/d\eta$  is the visibility function,  $\tau$  is the optical depth to Thomson scattering,  $\mathbf{p}_{\parallel} = (1 + \delta)\mathbf{v}_{\parallel}$ , with  $\delta$  the electron overdensity. We assume that  $g(\eta)$  doesn't change significantly in one redshift bin, and integrate  $\mathbf{p}_{\parallel}$  along radial axis to get  $\hat{\Theta}_{kSZ}$ .

(4) Calculate correlation coefficients.

We compare reconstructed kSZ signals  $\hat{\Theta}_{kSZ}$  with kSZ signals  $\Theta_{kSZ}$  directly from simulations. To quantify the tightness of correlation, we employ a quantity  $r$ :

$$r \equiv \frac{P_{recon,real}}{\sqrt{P_{recon}P_{real}}} \quad (7)$$

### III. SIMULATIONS

#### A. Simulation Set up

We use six  $N$ -body simulations from the CUBEP<sup>3</sup>M code [26], each evolving  $1024^3$  particles in a  $(1.2\text{Gpc}/h)^3$  box. We assume Hubble parameter  $h = 0.678$ , baryon density  $\Omega_b = 0.049$ , dark matter density  $\Omega_c = 0.259$ , amplitude of primordial curvature power spectrum  $A_s = 2.139 \times 10^{-9}$  at  $k_0 = 0.05 \text{ Mpc}^{-1}$  and scalar spectral index  $n_s = 0.968$ . We analyse the outputs at redshift 1 and 2.

To resemble realistic observations:

1. We import a cut off scale  $k_c$ , assume that modes with  $k > k_c$  are not resolved. This is reasonable for a filled aperture experiment, which has good brightness sensitivity and an exponentially growing noise at small scales. We choose

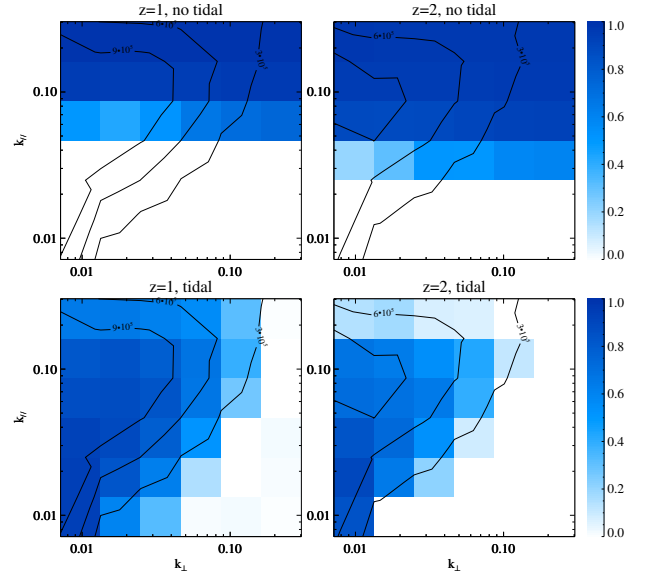


FIG. 1: (Top) The cross correlation  $r$  between  $P_{v_z}$  and  $P_{\hat{v}_z^{fs}}$  calculated from foreground subtracted field  $\delta_{fs}$ ; (Bottom) The cross correlation between  $P_{v_z}$  and  $P_{\hat{v}_z^{tide}}$  calculated from  $\hat{\kappa}_c$ . The contour line indicates  $k^3 P(k)$ .

$k_c = 0.5 h/\text{Mpc}$  and  $0.32 h/\text{Mpc}$  respectively for  $z = 1$  and  $z = 2$ , which corresponds to  $\ell \sim 1150$ . This is generally realistic, judging from ongoing 21cm experiments like CHIME [18][27] and Tianlai [28][19].

2. We use a high pass filter  $W_{fs}(k_{\parallel}) = 1 - e^{-k_{\parallel}^2 R_{\parallel}^2/2}$  to imitate the foreground subtraction. We choose  $R_{\parallel} = 15 \text{ Mpc}/h$  for  $z = 1$  and  $R_{\parallel} = 8 \text{ Mpc}/h$  for  $z = 2$ , which gives  $W_{fs} = 0.5$  at  $k_{\parallel} = 0.08 \text{ Mpc}/h$  and  $0.15 \text{ Mpc}/h$  respectively.

The observed 21cm field after foreground subtraction is then given by

$$\delta_{fs}(\mathbf{k}) = \delta(\mathbf{k}) W_{fs}(k_{\parallel}) \Theta(k_c - k), \quad (8)$$

where  $\delta(\mathbf{k})$  is the original density field,  $\Theta(x)$  equals 0 for  $x < 0$  and equals 1 elsewhere.

After that, we reconstruct the large scale fields  $\hat{\kappa}_c$  from  $\delta_{fs}$  via cosmic tidal reconstruction. We use  $\hat{\kappa}_c$  to obtain an estimate radial velocity field  $\hat{v}_z^{tide}$  follow Eq.(5). We reconstruct the kSZ signal  $\hat{\Theta}_{kSZ}$  following Eq.(6) and compare it with kSZ signal.

#### B. Results

##### 1. Correlation of reconstructed velocity fields:

We first present the result about reconstructed velocity field (Eq.(5)) in Fig.1. The upper two panels show the cross correlation  $r$  between  $v_z$  and  $\hat{v}_z^{fs}$  calculated from foreground subtracted field  $\delta_{fs}$ ; the lower panel shows the cross correlation between  $v_z$  and  $\hat{v}_z^{tide}$  calculated from  $\hat{\kappa}_c$ . The contour line represent the value of  $k^3 P(k)$ , which is related to the importance of each mode when generating kSZ signals.

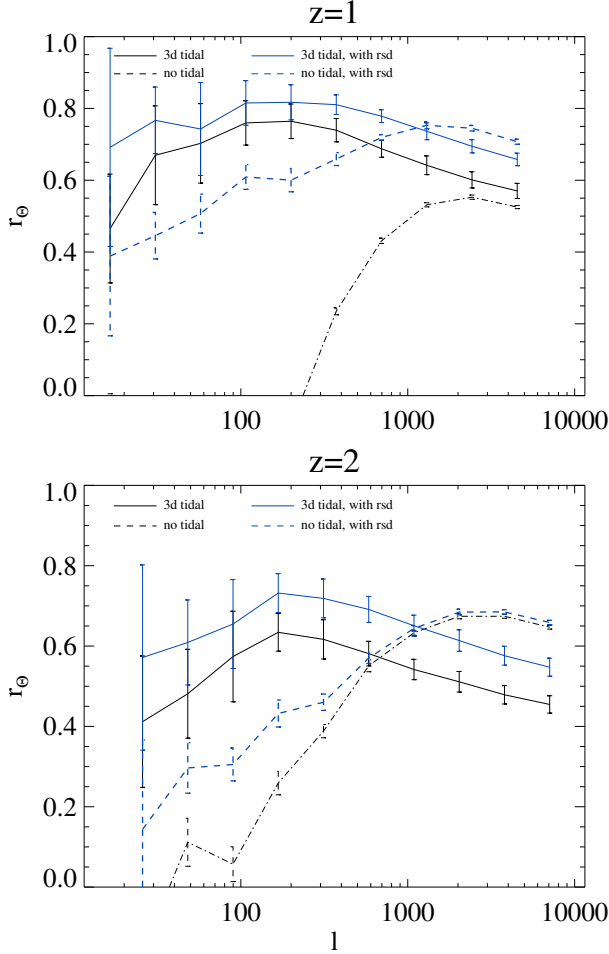


FIG. 2: The cross correlation  $r$  between reconstructed kSZ  $P_{\hat{\Theta}_{kSZ}}$  and real kSZ  $P_{\Theta_{kSZ}}$ . (Dashed line) kSZ calculated from foreground subtracted 21cm density field  $\delta_{fs}$ ; (Solid line) kSZ calculated from tidal reconstructed density field. (Blue lines) take into account of redshift distortions.

Notice: 1. Although the foreground at  $z=2$  is stronger, the non-linear effects are weaker. Therefore, we can still see some correlations at  $k_{\parallel} \lesssim 0.1$ , with the little density signals left. And these correlations are even better than the  $z=1$  case after the gaussianization.

On the other hand, there is degrading performance of tidal reconstruction on  $z=2$ . This is likely due to the stricter cutoff  $k_c = 0.32h/Mpc$  compared to  $k_c = 0.5h/Mpc$  at  $z=1$ .

2. Since tidal reconstruction relies strongly on large  $k$  modes, and we only lost small  $k_z$  modes in the foreground (Fig.1 upper panel). The reconstruction on  $k_{\parallel}$  is better than on  $k_{\perp}$ , which is an advantage for estimating  $v_z$ .

Important to see: 1. The previously lost small  $k_{\parallel}$  modes has been well reconstructed through the 3D tidal reconstruction procedures. 2. The modes recovered in tidal reconstruction play more vital role in generating kSZ signals.

2. Correlation of reconstructed kSZ signals:

In Fig.2, we demonstrate the correlation  $r$  between the reconstructed kSZ signal  $\hat{\Theta}$  and original kSZ signal  $\Theta$  (black lines). We used both original foreground subtracted density

field and tidal reconstructed density field and compare the different results.

Important to see: 1. For  $z=1$ , there are significant improvement on the cross-correlation after tidal reconstruction, especially below  $l \sim 2000$ . 2. For  $z=2$ , the tidal reconstruction improves the cross-correlation for  $l \lesssim 800$ . However, since the non-linear effect is less strong at this stage, the original 21cm density field is good enough to reconstruct kSZ signal for  $l \gtrsim 800$ . Combining them, we would have good cross-correlation for  $l \sim 20 - 8000$ .

In all, for both redshift, with the non-ideal foregrounds and resolutions we assume, we are able to obtain a correlation  $r \gtrsim 0.5$  for  $l \sim 50 - 5000$  between 21cm density field and kSZ signals.

## IV. ERROR AND DISCUSSION

### A. Statistical Error

We use the statistical error to estimate the S/N ratio for real surveys. Taking into account the contamination from primary CMB and facility noises, it can be approximated as:

$$\frac{\Delta C_l}{C_l} \simeq \frac{1}{r \sqrt{(2l+1)\Delta l f_{sky}}} \sqrt{\frac{C_l^{CMB} + C_l^{kSZ, \Delta z} + C_l^{CMB, N}}{C_l^{kSZ, \Delta z}}} \quad (9)$$

Where  $C_l^{CMB}$  is the angular powerspectrum of primary CMB;  $C_l^{CMB, N}$  indicates the facility noises;  $C_l^{kSZ, \Delta z}$  is the kSZ signal from a certain redshift bin;  $r$  is the correlation coefficients we get;  $f_{sky}$  is the percent of sky area covered by both surveys.

In our case, we calculate  $C_l^{CMB}$  from CAMB [29]. We use Planck 2015 results [30] at 217GHz to estimate  $C_l^{CMB, N}$ .  $C_l^{CMB, N} = (\sigma_{p,T} \theta_{FWHM})^2 W_l^{-2}$ ; where  $\sigma_{p,T} = 8.7 \mu K_{CMB}$  is Sensitivity per beam solid angle,  $\theta_{FWHM} \sim 5'$  is the effective beam FWHM,  $W_l = \exp[-l(l+1)/2l_{beam}^2]$  is the smoothing window function, with  $l_{beam} = \sqrt{8 \ln 2} / \theta_{FWHM}$ . We choose  $f_{sky} = 0.8$ , since it is feasible for 21cm intensity mapping to survey large sky areas. We choose  $\Delta l/l = 0.1$ . And for  $C_l^{kSZ, \Delta z}$ , we choose two bins of size 1200 Mpc/h, centered at redshift 1,2 respectively.

In Fig.3, we plot the S/N level for the two redshift bins. The S/N will exceeds 3 from  $l \sim 500 - 3000$ .

Since we only use the correlation calculated from tidal reconstructed field, the S/N shall be higher for  $z=2$  combining tidal reconstructed field and foreground subtracted field. Moreover, since  $C_l^{kSZ}$  is relatively flat, it is possible to bin it into larger  $\Delta l$ . eg. [17] choose  $\Delta l = 200$ , and this will yield better S/N for  $l < 2000$  in Fig.3.

What's more, Planck's noise level is far from ideal. If we consider the case of 4th generation facilities, there will also be a giant leap for S/N at large  $l$ . However, in that case, we have to have accurate subtraction for CMB lensing, when primary CMB dims out.

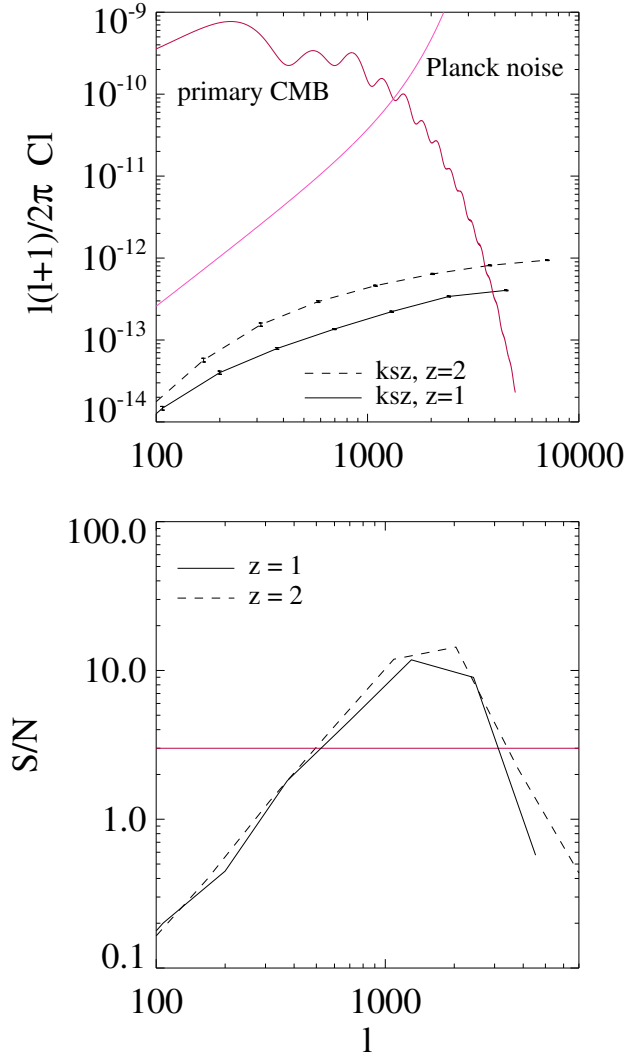


FIG. 3: (Top) Relative strength of kSZ signal, within a box of  $\Delta\chi = 1200 Mpc/h$ . (Bottom) predicted S/N, assuming Planck noise,  $\Delta l/l = 0.1$ ,  $f_{sky} = 0.8$ .

## B. Redshift Distortion

## V. CONCLUSION

## VI. ACKNOWLEDGE

We acknowledge discussions with Kendrick Smith, Matthew Johnson, Wenkai Hu, Tianxiang Mao and Jiawei Shao. The simulations were performed on the BGQ supercomputer at the SciNet HPC Consortium. SciNet is funded by: the Canada Foundation for Innovation under the auspices of Compute Canada; the Government of Ontario; the Ontario Research Fund – Research Excellence; and the University of Toronto. Research at the Perimeter Institute is supported by the Government of Canada through Industry Canada and by the Province of Ontario through the Ministry of Research Innovation. The Dunlap Institute is funded through an endowment established by the David Dunlap family and the University of Toronto.

- 
- [1] R. J. Cooke, M. Pettini, R. A. Jorgenson, M. T. Murphy, and C. C. Steidel, *ApJ* **781**, 31 (2014), 1308.3240.
  - [2] G. Hinshaw, D. Larson, E. Komatsu, D. N. Spergel, C. L. Bennett, J. Dunkley, M. R. Nolta, M. Halpern, R. S. Hill, N. Odegard, et al., *ApJS* **208**, 19 (2013), 1212.5226.
  - [3] E. Komatsu, K. M. Smith, J. Dunkley, C. L. Bennett, B. Gold, G. Hinshaw, N. Jarosik, D. Larson, M. R. Nolta, L. Page, et al., *ApJS* **192**, 18 (2011), 1001.4538.
  - [4] G. Hinshaw, D. Larson, E. Komatsu, D. N. Spergel, C. L. Bennett, J. Dunkley, M. R. Nolta, M. Halpern, R. S. Hill, N. Odegard, et al., *ApJS* **208**, 19 (2013), 1212.5226.
  - [5] A. M. Soltan, *A&A* **460**, 59 (2006), astro-ph/0604465.
  - [6] M. Fukugita and P. J. E. Peebles, *ApJ* **616**, 643 (2004), astro-ph/0406095.
  - [7] J. K. Werk, J. X. Prochaska, J. Tumlinson, M. S. Peeples, T. M. Tripp, A. J. Fox, N. Lehner, C. Thom, J. M. O’Meara, A. B. Ford, et al., *ApJ* **792**, 8 (2014), 1403.0947.
  - [8] R. Davé, B. D. Oppenheimer, N. Katz, J. A. Kollmeier, and D. H. Weinberg, *MNRAS* **408**, 2051 (2010), 1005.2421.
  - [9] R. A. Sunyaev and Y. B. Zeldovich, *Comments on Astrophysics and Space Physics* **4**, 173 (1972).
  - [10] R. A. Sunyaev and I. B. Zeldovich, *MNRAS* **190**, 413 (1980).
  - [11] P. Zhang, U.-L. Pen, and H. Trac, *MNRAS* **347**, 1224 (2004), astro-ph/0304534.
  - [12] M. McQuinn, S. R. Furlanetto, L. Hernquist, O. Zahn, and M. Zaldarriaga, *ApJ* **630**, 643 (2005), astro-ph/0504189.
  - [13] O. Zahn, C. L. Reichardt, L. Shaw, A. Lidz, K. A. Aird, B. A. Benson, L. E. Bleem, J. E. Carlstrom, C. L. Chang, H. M. Cho, et al., *ApJ* **756**, 65 (2012), 1111.6386.
  - [14] N. Hand, G. E. Addison, E. Aubourg, N. Battaglia, E. S. Battistelli, D. Bizyaev, J. R. Bond, H. Brewington, J. Brinkmann, B. R. Brown, et al., *Physical Review Letters* **109**, 041101 (2012), 1203.4219.
  - [15] J. Shao, P. Zhang, W. Lin, Y. Jing, and J. Pan, *MNRAS* **413**,

- 628 (2011), 1004.1301.
- [16] M. Li, R. E. Angulo, S. D. M. White, and J. Jasche, *MNRAS* **443**, 2311 (2014), 1404.0007.
  - [17] J. C. Hill, S. Ferraro, N. Battaglia, J. Liu, and D. N. Spergel, *ArXiv e-prints* (2016), 1603.01608.
  - [18] K. Bandura, G. E. Addison, M. Amiri, J. R. Bond, D. Campbell-Wilson, L. Connor, J.-F. Cliche, G. Davis, M. Deng, N. Denman, et al., in *Society of Photo-Optical Instrumentation Engineers (SPIE) Conference Series* (2014), vol. 9145 of *Society of Photo-Optical Instrumentation Engineers (SPIE) Conference Series*, p. 22, 1406.2288.
  - [19] Y. Xu, X. Wang, and X. Chen, *ApJ* **798**, 40 (2015), 1410.7794.
  - [20] <http://www.acru.ukzn.ac.za/hirax/>.
  - [21] U.-L. Pen, R. Sheth, J. Harnois-Déraps, X. Chen, and Z. Li, *ArXiv e-prints* (2012), 1202.5804.
  - [22] H.-M. Zhu, U.-L. Pen, Y. Yu, X. Er, and X. Chen, *ArXiv e-prints* (2015), 1511.04680.
  - [23] T. Di Matteo, B. Ciardi, and F. Miniati, *MNRAS* **355**, 1053 (2004), astro-ph/0402322.
  - [24] K. W. Masui, E. R. Switzer, N. Banavar, K. Bandura, C. Blake, L.-M. Calin, T.-C. Chang, X. Chen, Y.-C. Li, Y.-W. Liao, et al., *ApJ* **763**, L20 (2013), 1208.0331.
  - [25] E. R. Switzer, T.-C. Chang, K. W. Masui, U.-L. Pen, and T. C. Voytek, *ApJ* **815**, 51 (2015), 1504.07527.
  - [26] J. Harnois-Déraps, U.-L. Pen, I. T. Iliev, H. Merz, J. D. Emberson, and V. Desjacques, *MNRAS* **436**, 540 (2013), 1208.5098.
  - [27] L. B. Newburgh, G. E. Addison, M. Amiri, K. Bandura, J. R. Bond, L. Connor, J.-F. Cliche, G. Davis, M. Deng, N. Denman, et al., in *Society of Photo-Optical Instrumentation Engineers (SPIE) Conference Series* (2014), vol. 9145 of *Society of Photo-Optical Instrumentation Engineers (SPIE) Conference Series*, p. 91454V, 1406.2267.
  - [28] X. Chen, *International Journal of Modern Physics Conference Series* **12**, 256 (2012), 1212.6278.
  - [29] A. Lewis, A. Challinor, and A. Lasenby, *Astrophys. J.* **538**, 473 (2000), astro-ph/9911177.
  - [30] Planck Collaboration, R. Adam, P. A. R. Ade, N. Aghanim, M. Arnaud, M. Ashdown, J. Aumont, C. Baccigalupi, A. J. Banday, R. B. Barreiro, et al., *ArXiv e-prints* (2015), 1502.01587.